Distribution Agreement

In presenting this thesis as a partial fulfillment of the requirements for a degree from Emory University, I hereby grant to Emory University and its agents the non-exclusive license to archive, make accessible, and display my thesis in whole or in part in all forms of media, now or hereafter know, including display on the World Wide Web. I understand that I may select some access restrictions as part of the online submission of this thesis. I retain all ownership rights to the copyright of the thesis. I also retain the right to use in future works (such as articles or books) all or part of this thesis.

Alexander David Savello April 14, 2011

Observations and Models of the Eclipsing Binary System KR Persei

by

Alexander David Savello

Dr. Richard Williamon
Adviser

Department of Physics

Dr. Richard Williamon

Adviser

Horace Dale

Committee Member

Dr. Scott Stewart

Committee Member

April 14, 2011

Observations and Models of the Eclipsing Binary System KR Persei

By

Alexander David Savello

Dr. Richard Williamon

Adviser

An abstract of
a thesis submitted to the Faculty of Emory College of Arts and Sciences
of Emory University in partial fulfillment
of the requirements of the degree of
Bachelor of Sciences with Honors

Department of Physics

2011

ABSTRACT

KR Persei (KR Per) [RA: 04 37 09, Dec: +44 12 40 JD 2000], a detached eclipsing binary star system located in the constellation Perseus, is the subject of this thesis. Previous research performed on KR Per, conducted in 1985 by Chen et. al, identified various astronomical quantities for KR Per. While Chen et. al appear to have calculated many astronomical parameters, reevaluation using newer models in this current study suggests not all may be accurate. Based on the observations performed at Emory University in Atlanta, GA, USA, from September 2010 to February 2011, KR Per does not appear to have an eccentricity of 0.009 or a longitude of periastron of 160^{o}. Furthermore, the stellar classification of both components as F5V appears to be inaccurate and a stellar classification of G8 seems more likely. Finally, there is a strong possibility of a multiple reflection effect in KR Per determined by non-standard shoulder regions of the light curves. If this multiple reflection effect does exist, the primary component must have a large convective zone, while the secondary star must have a large radiative zone.

Observations and Models of the Eclipsing Binary System KR Persei

By

Alexander David Savello

Dr. Richard Williamon

Adviser

A thesis submitted to the Faculty of Emory College of Arts and Sciences
of Emory University in partial fulfillment
of the requirements of the degree of
Bachelor of Sciences with Honors

Department of Physics

2011

ACKNOWLEDGEMENTS

I would like to express my sincere gratitude and thanks to Horace Dale for his continuous support of my honors study and research, for his patience, motivation, understanding, and vast knowledge. His expertise on variable stars was invaluable in the research and writing of this thesis. Despite having a newborn at home, Horace spent many nights in the Observatory collecting data with me, in addition to reviewing and discussing data analysis in BM3 and PERANSO. I could not have imagined having a more approachable mentor for my honors study.

My sincere thanks go to Dr. Williamon for being a calm yet enthusiastic advisor for this honors project. Dr. Williamon always kept his door open and supported me through endless questioning sessions about my thesis. After teaching my Astrophysics I and II classes, he entrusted me to TA several of his courses where I learned how to teach younger students about astronomy. I came to Emory to study and excel in astrophysics and his knowledge and guidance allowed me to do just that.

My thanks to Dr. Stewart for serving on my thesis committee and for being my advisor for the Emory Honor Council. His guidance and candidness made the Honor Council experience rewarding and helped me negotiate my way through the procedures and negotiations.

Finally, I would like to thank the Emory University Physics Department for the high quality instrumentation, coursework, and for supporting my training and research during my four years at Emory.

TABLE OF CONTENTS

1 Introduction 1

2 Binary Star Systems and Astronomical Measurements 3

Observations and Classifications of Binary Star Systems 3

Astronomical Quantities 5

Physical Classifications of Binary Systems 6

Naming Conventions 7

Stellar Spectra and Radial Velocity Curves 8

Phases of Variable Star's Orbit 9

Stellar Classification and HR Diagram 10

Measuring Brightness 11

Measuring Time 11

Time of Minima and O-C Diagram 12

3 Observational Methods and Photometry 13

Observational Methods 13

Johnson/Bessel Filter Set 15

Photometry 16

4 Observations of KR Persei 17

Research Background 17

Observations 17

Minimum Timings and O-C Diagram 19

Results 23

Light Curve and Modeling 24

5 Discussions and Conclusions 32

References 39

LIST OF FIGURES

1 Eclipsing Binary Illustration 4
2 Classification of Binary Systems 6
3 Spatial Identification of Lagrangian Points 7
4 Hertzsprung-Russel Diagram 10
5 Cassegrain Telescope Diagram 13
6 Johnson/Bessel UBVRI Filters 15
7 Starfield of KR Persei 18
8 KR Per O-C Diagram 22
9 KR Per Geometric Model 25
10 KR Per 3D Model 26
11 KR Per IRVB Light Curves 27
12 KR Per B Light Curve without reflection effect 28
13 KR Per B Light Curve with reflection effect 28
14 KR Per V Light Curve without reflection effect 29
15 KR Per V Light Curve with reflection effect 29
16 KR Per R Light Curve without reflection effect 30
17 KR Per R Light Curve with reflection effect 30
18 Reflection Values vs. Wavelength 31
19 Planck Distribution 35
20 KR Per 3D Spot Model 37
21 KR Per V Light Curve with Spot modeling 37

LIST OF TABLES

1 KR Per Observed Times of Minimum 19
2 KR Per Observed Minus Calculated Times 20
3 KR Per Period Length by Dataset 23
4 KR Per Orbital Parameter Solutions – Chen et. al 24
5 KR Per Orbital Parameter Solutions – All Datasets 24
6 Parameters for Figure 13 28
7 Parameters for Figure 15 29
8 Parameters for Figure 17 30

1 – INTRODUCTION

Over half of the stars in the galaxy occur in pairs or multiples. A star system with only two stars, a binary system, is a system where the two stars orbit one another around a common center of mass. Extensive astronomical data can be obtained from binary star systems because it is possible to identify the exact orbital period (the time it takes for the stars to complete one revolution about the center of mass). Using observational data, it is possible to extrapolate more complex information about the star system, such as each star's mass, color, size, and density. Furthermore, by identifying this information, binary stars can be used as standards to understand and obtain fundamental values for non-binary stars. For example, when mass or size data is obtained on a single star system, those values can be compared to the known values from a binary system and exact measurements can be calculated. Therefore, without binary star systems, scientists would not have a stellar baseline by which multiple star systems (three or more stars orbiting) and single star systems can be understood (Carroll and Ostlie 2007: 180-182) (Coughlin 2007: 1-2).

KR Persei [RA: 04 37 09, Dec: +44 12 40 JD 2000][1] is a binary star system located in the constellation Perseus and is the focus of this thesis. The most recent research performed on KR Persei was completed in 1985 by Dr. Richard Williamon at the Fernbank Observatory in Atlanta, Georgia, USA and Dr. Kwan-Yu Chen at the Yunnan Observatory in Kunming, Yunnan, China. These two scientists identified many astronomical quantities for KR Persei including the period, viewing inclination, spectral classification, temperature, mass ratio, and radii of the two stars. The hope is either to confirm or improve their 25-year-old conclusions or to offer new insights into the physical characteristics of this binary.

[1] RA = Right Ascension, Dec = Declination. These values are the coordinates of KR Persei in the night sky with the epoch being JD2000.

In section 2 of this thesis, I present a thorough introduction to binary star systems and the different astronomical quantities that can be calculated from telescopic observation. Section 3 discusses the observational methods and photometry used to acquire these quantities for KR Persei. Section 4 outlines previous analysis of KR Persei by Chen et al. and presents findings from my own observations and analysis. Finally, Section 5 provides discussions and conclusions where my results are interpreted and compared to the 1985 work of Chen et al.

2 – Binary Star Systems and Astronomical Measurements

Observational Classifications of Binary Star Systems

Binary star systems are identified as having a primary and a secondary star that both can be observed, directly or indirectly. The primary star is the hotter star while the secondary is the cooler star. There are four main classifications of binary star systems, each named after the scientific method of discovery: Spectroscopic observation, visual observation, astrometric observation, and eclipsing observation[2].

Spectroscopic binaries are identified by looking at the Doppler Effect on the light emitted by the stars. As Star A moves towards Earth in its orbit, its light spectra shifts towards the blue. Meanwhile, Star B is moving away from the Earth so its light spectra shifts towards the red. The amount of blue shift or red shift can be quantified and astronomical quantities can be identified.

Visual binaries are star systems in which the angular separation between the two bodies is large enough that it is possible to see the two stars individually in a telescope. However, unlike optical doubles, visual binary systems *do* interact gravitationally and this gravitational interaction is usually verified by one of the other methods of binary observation.

Astrometric binaries are stars that show no signs of orbiting one another but do seem to orbit a common center of mass in empty space. Since no relative motion can be seen between the two stars, astronomers use background stars in the field to identify any movement of the foreground stars in question. Using this mathematical modeling, it is possible to identify binary systems that may have very long orbits.

---

[2] Binary star systems have been confused with "optical doubles", but are not alike. Optical doubles are two stars that simply lie along the same line of sight and appear to be interacting, but in fact do not – a large physical separation between the two stars and lack of gravitational interaction separate these phenomena from binary systems

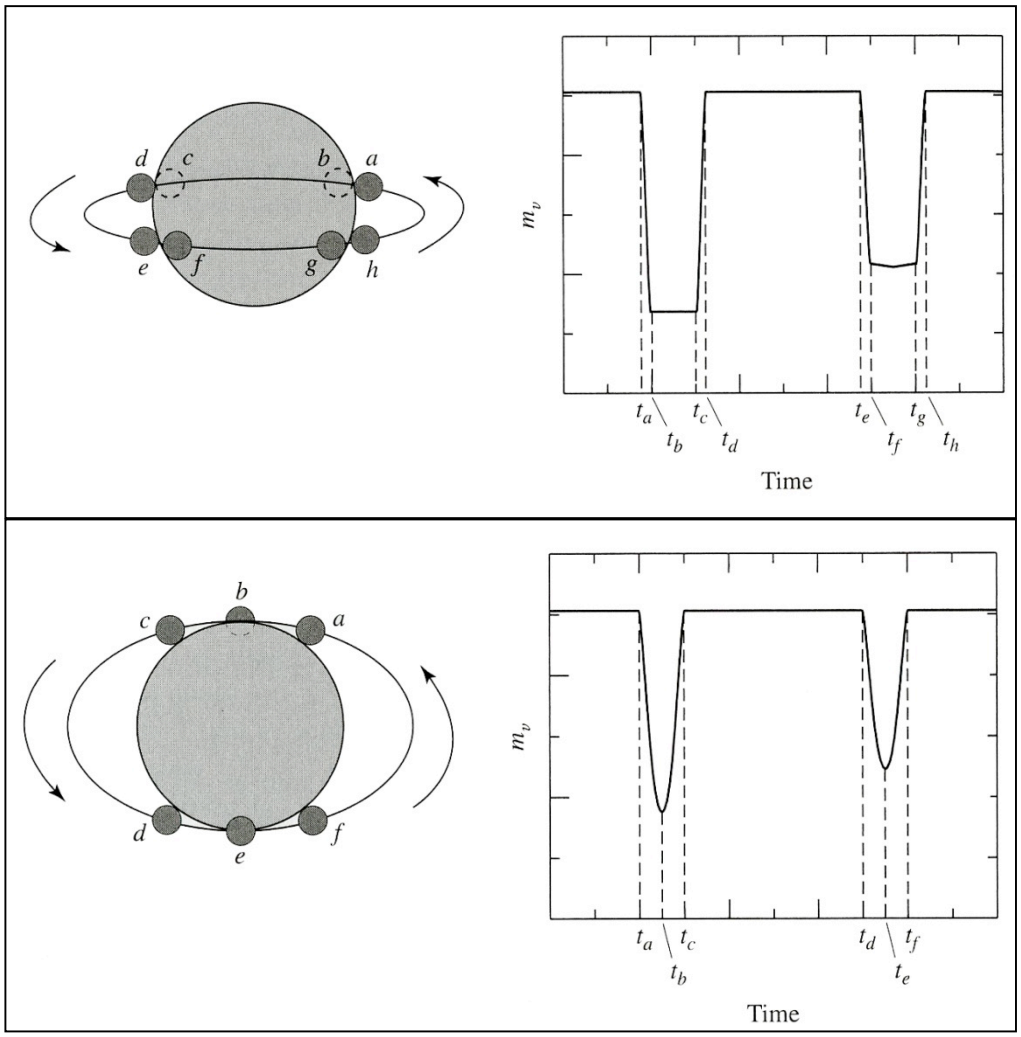

Figure 1: Simplistic rendition of a potential light curve for a partial eclipsing binary system. The top diagram is for a total eclipsing binary system while the bottom is a partial eclipse. The beginning of primary eclipse is labeled as t_a with primary minimum at t_b. t_c to t_d is the shoulder of the light curve where neither star's light is blocked. Secondary eclipse begins at t_d and secondary minimum at t_e. The smaller star is the primary (Carroll and Ostlie 2007: 190).

The final type of binary star system is the eclipsing binary (also known as an extrinsic variable star), which is the subject of this thesis. These stars lie on a plane that is oriented such that, when viewed from Earth, the two stars appear to eclipse each other during their orbit. These star systems are not like visual binaries because their orbits are so close together; the star systems appear as point sources even though there are two stars present. However, it is possible to identify the individual stars because the amount of light received by Earth is periodically

changing due to the eclipsing nature of their orbits. This change in light received by Earth over the course of the entire orbit of the stars is called a light curve. Figure 1 shows a simplistic rendition of a total and partial eclipsing binary star system with its corresponding light curve. When the hotter primary star is eclipsed by the cooler secondary, the dip in the light curve is called the *primary minimum*, and when the primary star passes in front of the secondary, the dip is called the *secondary minimum*. By studying the light curve, it is possible to obtain many astronomical quantities about the binary star system (Carroll and Ostlie 2007: 180-182).

Astronomical Quantities

The specific astronomical quantities that can be obtained from the photometry and spectroscopy of a binary star system include the period (time to complete one orbit, P), mass ratio of the system (m_s/m_p), radius of each star (r_s and r_p), surface temperature of each star (T_s, T_p), ratio of primary and secondary eclipse depths, and viewing inclination of the system (i).

The period can be directly observed using a system's light curve. The orbital separation is the distance between each star and the common center of mass. The mass ratio of the system is the mass of one star divided by the mass of the other. The radii of the stars correlate with the mass of the star and depend on the width of the minimums on the light curve. The depth of the primary and secondary minima can be used to determine the surface temperature of the stars, according to Stephan-Boltzman's Law[3]. Finally, if a binary star system has an inclination of 90 degrees it is said be viewed "exactly edge on" and if it has an inclination of 0 degrees it is being viewed "face-on" and no eclipsing will be seen. The lower the inclination, the shallower the primary and second minima in the light curve will be (Carroll and Ostlie 2007:183-195).

[3] States that the total energy radiated per unit surface per unit time from a blackbody is proportional to the fourth power of the blackbody's temperature ($L = \sigma T^4$).

Physical Classifications of Binary Systems

Binary star systems also have physical classifications that are determined by how large or small each star is in three-dimensional space. The stars atmosphere can partially, completely, or overly fill this three-dimensional space, called the Roche lobe. When the Roche lobes for each star are combined, they form teardrop-shaped regions of space that separate the two stars from one another by an equipotential surface (points in space that share the same value of gravitational potential).

Inside these regions, matter is gravitationally bound to the star in that lobe but if the star expands outside of that lobe, the matter can escape the gravitational pull of its star. If both stars are inside their respective Roche lobes but not physically interacting, the system is detached (Figure 2a). If one star fills its Roche lobe, then matter from the smaller star will flow to its companion by through a point in space where the combined gravitational pull from both stars is zero (called a Lagrangian point) and is classified as semi-detached (Figure 2b). If both stars are as large as, or larger than their respective Roche lobe, their surfaces are physically in contact with one another and the system is classified as a contact system (Figure 2c). In a contact system, a dumbbell-shaped atmosphere of the contacted stars encompass Lagrangian point L_2 as well (Carroll and Ostlie 2007: 658).

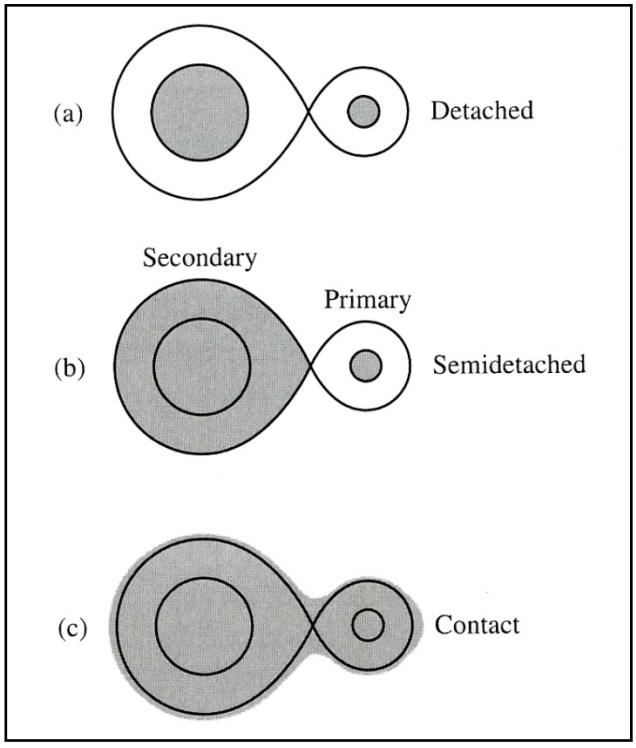

Figure 2: Classification of binary systems with their respective Roche lobe. (a) Detached. (b) Semidetached. (c) Contact (Carroll and Ostlie 2007: 659).

Every binary star system has five Lagrangian points where small objects (like a satellite) will remain stationary relative to the two stars. At these points, the combined gravitational pull from both stars counteracts one another and the net force on the satellite or object is zero. These points are represented in Figure 3 as L_1 to L_5 (Carroll and Ostlie 2007: 655-657).

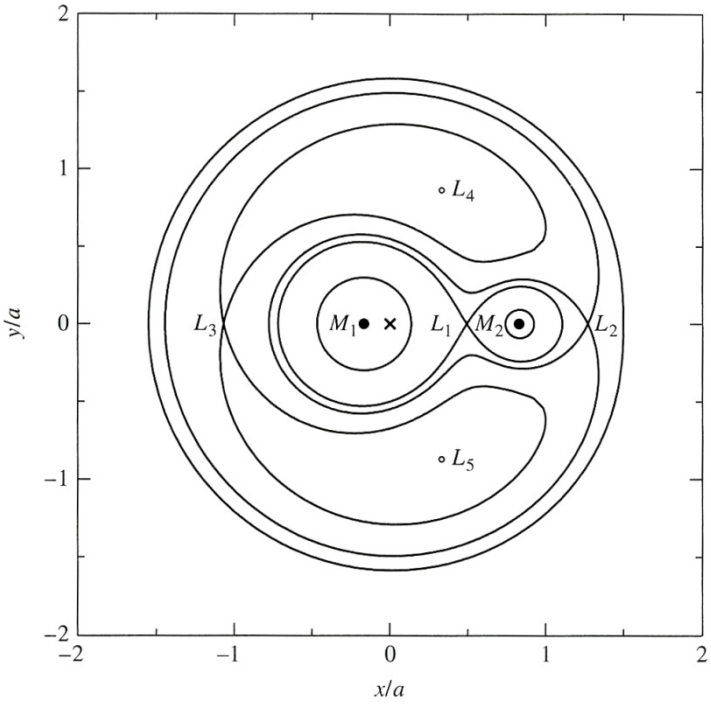

Figure 3: Spatial identification of the five Lagrangian points around a binary star system. M_1 is primary star and M_2 is secondary star (Carroll and Ostlie 2007: 657)

Naming Conventions

In order to create a comprehensive catalog of variable stars, a naming convention was created so that astronomers can easily identify the variable star based on their location in the sky and date of discovery. The first variable star found in a constellation is given the letter R, followed by the genitive form of the constellation name. For example, *R Ceti* would be the first variable star found in the constellation Cetus. The next variable star found in Cetus would be *S*

Ceti, followed by *T Ceti*, and so on, until *Z Ceti*. If any more variable stars were found in a specific constellation after Z, astronomers would switch to a two-letter naming convention before the constellation name, beginning with RR (and followed by RS, RT…SS, ST, SU, etc.). If still more variable stars were discovered in Cetus, astronomers would go back to the beginning of the alphabet and use AA, AB, AC, AD, and so on. The letter "J" is not used in this classification, to avoid confusion with "I". If all the two-letter designations were used up in a specific constellation (334 possible designations), numerical designations would be employed as needed (V335 Ceti, V336 Ceti, etc.) (Coughlin 2007: 3-4).

Stellar Spectra and Radial Velocity Curves

A stellar spectrum is light separated by a prism such that intensity is plotted with respect to wavelength. This plot reveals information about a variable star that is not possible to obtain with a light curve alone. For example, each element in a star will create specific light bands on a spectrum; taken together, these bands indicate the elemental composition of the star. Furthermore, the width of each band may give an indication of the density, temperature, and surface gravity of the star.

Radial velocity curves are derived from a star's spectrum and are necessary to compile a complete understanding of a binary star system. Radial velocity is the calculated motion of a star as it moves towards or away from the observer, identified by recording the shift of a star's spectrum as it shifts between shorter and longer wavelengths (Doppler Shift). Once it is known what the exact Doppler Shift of the system is relative to the rest wavelengths, the velocity of each component can be quantified.

While light curves can be used to determine the temperature distribution and relative size of each component, radial velocity curves are needed to determine each component's mass.

Phases of a Variable Star's Orbit

When astronomers refer to specific times in a variable star's orbit, units of phase are used, with zero to one representing a complete orbit.

Phase of 0 – Primary star is being eclipsed by the secondary (primary eclipse)

Phase of 0.5 – Primary star is eclipsing secondary star (secondary eclipse)

Phase of 0.25 and 0.75 – system is out of eclipse and referred to as the shoulders of the light curve

Stellar Classification and the HR Diagram

The simplest way of classifying the many different sizes, temperatures, luminosities, and colors of stars is using the Harvard spectral classification and the Morgan Keenan system of stellar classification in combination. Individual stars are classified based on their color and temperature in the star's upper atmosphere using the letters **O**, **B**, **A**, **F**, **G**, **K**, and **M** where the hottest stars are O-type stars and the coolest are M-type stars. A number (**0** to **9**) is appended to the letter designation to indicate tenths of the range between different stellar classes. For example, a G5 type star is five-tenths hotter than a K0 and five-tenths cooler than a F0 star. Also note that, within the same classification, lower-numbered stars are hotter. Finally, a Roman numeral is added to the designation, from **I** to **V,** where I (subdivided into Ia and Ib) denote a supergiant star and V represents a main-sequence star. For example, our Sun is a G2V type star (5777 K, main sequence).

This classification system allows astronomers both to accurately categorize all stars in the night sky and to locate a star's position on an easy to interpret diagram called the Hertzsprung-Russel diagram (H-R diagram). The Hertzsprung-Russel diagram depicts the relationship between a star's luminosity, spectral classification, and temperature (Figure 4). Most stars

occupy the *main sequence* band of the diagram while a smaller number of stars are classified as *supergiants*, *giants*, and *white dwarfs* (Carroll and Ostlie 2007: 219-228).

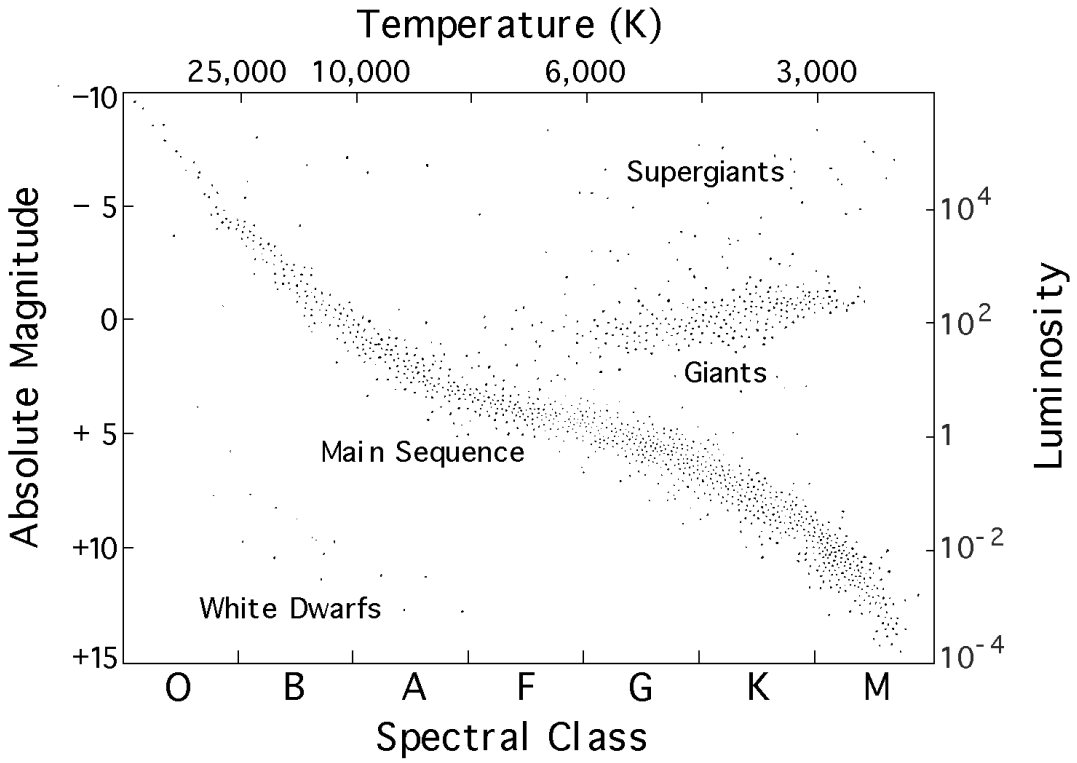

Figure 4: The Hertzsprung-Russel diagram. A star's location on the diagram can be identified using the star's Spectral Class, Absolute Magnitude, Luminosity, and Temperature (K). The star's location on the diagram identifies it as one of four types of stars: Supergiant, Giant, Main Sequence, or White Dwarf (Goddard Space Flight Center 2011).

A main sequence star is one that is most stable and is actively fusing hydrogen into helium in its core. Stars that have a greater luminosity on the main sequence curve have shorter lifespans (less than 5 billion years) and are usually very large (e.g. blue giant stars, classification O). Main sequence stars that have a lower luminosity are lower on the curve and usually are smaller redder stars that live for tens of billions of years.

Giant and supergiant stars are actively fusing helium or heavier elements in the core and burning hydrogen in the upper atmosphere. These are very massive stars that are usually red,

yellow, or orange in color due to their relatively low atmospheric temperature. Giants and supergiants are stars that are at the end of their life and die as either a supernova or white dwarf.

Finally, white dwarfs are stars that occupy the bottom left corner of the H-R diagram. These stars are very small and undergo no fusion but remain at very high temperatures as they enter what is thought to be one of the final stages of a star's life. As time goes by, the star will slowly emit less and less light and the temperature of the atmosphere will drop. Therefore, the spectral class of a white dwarf will gradually cool from a hot O-type star to a cool M-type (Carroll and Ostlie 2007: 219-224).

Measuring Brightness

Brightness is measured using a backwards-logarithmic scale called magnitude. Brighter objects have lower magnitudes and dimmer objects have higher ones. The zero point on the magnitude scale is the brightness of the star *Vega*. The logarithmic scale indicates that an object with a magnitude of five will be one hundred times dimmer than an object with a magnitude of zero. The two brightest objects in the sky, the Sun and a full moon, have apparent magnitudes of -26.74 and -12.74, respectively[4] (Carroll and Ostlie 2007: 60).

Measuring Time

Astronomers do not use the customary twenty-four hour clock and the Gregorian calendar when obtaining and cataloging astronomical data. Instead, astronomers record data in Heliocentric Julian Date (HJD). The Julian Date (JD) is the amount of time that has passed, in sidereal days, from noon Universal Time (UT) on January 1, 4713 BC (Universal Time is synonymous with Greenwich Mean Time).

[4] Another method of determining brightness is flux, which is simply a relative unit that is linear (maximum flux = 1) and will be used later in this thesis to compare data

Heliocentric Julian Date (HJD) is used to correct for the change in the Earth's position as it orbits the sun. This means that the distance from the Earth to an astronomical object can vary by up to two Astronomical Units (AU)[5]. When the Earth is on the far side of the sun relative to the object, the light from the object must travel an additional sixteen light-minutes[6] to reach Earth. Therefore, HJD is used to account for this extra time that the light must travel (Carroll and Ostlie 2007: 14-15).

Time of Minima and O-C Diagram

A time of minima is the exact moment at which the light curve reaches minimum light for both primary eclipse and secondary eclipse. By identifying the time of minima on multiple observing sessions, it is possible to see if the period is changing from session to session and by what amount. The period can change over time due to mass transfer between the two stars (in a semidetached or contact system), a third body perturbing the orbit of the binary stars, or magnetic spots (like our Sun's sunspots) on one or both of the stars.

An O-C Diagram is used to see if the actual observed time of minima (O) of a binary star system agrees with the calculated time of minima (C). The diagram has time as the x-axis (in HJD or epoch) and observed time of minima subtracted by calculated time of minima as the y-axis[7]. This Observed – Calculated (O-C) value can identify if the mathematical model and observed model of the binary system are in agreement. If the O and C models agree perfectly, then the slope of the line formed will be zero. But if a period of a binary system is changing, the O-C diagram will be curved (Coughlin 2007: 14-15).

---

[5] An AU is the average distance between the Earth and the Sun (approximately 149 million kilometers).

[6] Distance light travels in one minute

[7] The epoch is the amount of time that has passed since a specific time that can be used as a reference point for the period of a binary star system.

3 – Observational Methods and Photometry

Observational Methods

In order to collect enough light to see binary stars eclipse one another, a large telescope with an attached camera is needed. Being in the Atlanta area, light pollution is a main concern, as fainter magnitude stars can be difficult to observe. Therefore, the main instrument used in this project is the Emory University DFM Cassegrain telescope located on top of the Math and Science Center [N 33^o 47' 25.02", W 84^o 19' 36.6"] at an elevation of 297 meters. The telescope has a 24-inch primary mirror[8] and the larger the light collecting area, the fainter the objects that can be observed. To put this in perspective, a 24-inch telescope has 360,000 times the light collecting area of the human eye[9].

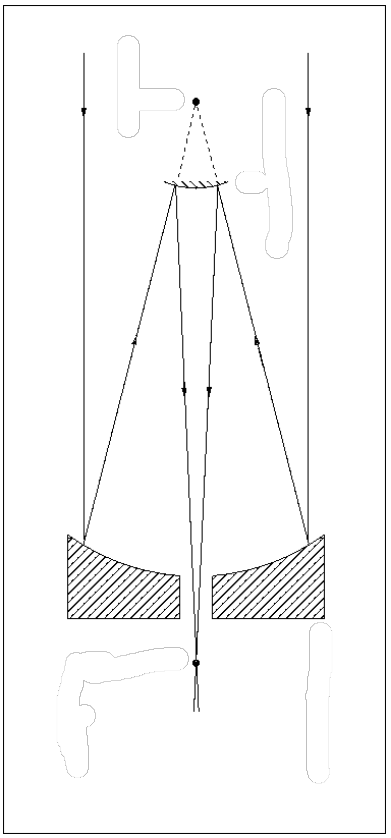

Figure 5: A ray diagram of a Cassegrain telescope. The primary mirror is located at the bottom of the tube, while the secondary mirror is located in the center of the diagram. The light is then focused to an eyepiece or camera (Dhillon 2010).

Cassegrain telescopes collect light through a light-collecting tube and reflect that light off of a primary mirror located at the bottom of the enclosure. The light is redirected to converge on a secondary mirror located back on the top of the telescope. This secondary mirror then reflects the light back down through a hole in the primary mirror, where it is focused in an eyepiece or CCD camera (Figure 5).

[8] The light-collecting area of the telescope

[9] This is assuming the human pupil is ~10mm in diameter and the Emory telescope has a diameter of 6000mm (24 inches). The light collecting area is proportional to the square of the diameter. Since the diameter of the Emory telescope is 600 times larger, the light collecting area is 600^2 or 360,000.

This project used two different cameras, the Apogee AP47 and the SBIG ST10 XME. These Charged-Coupled Device (CCD) cameras collect light over a user-defined period of time, which can range anywhere from a fraction of a second to many hours of integration. When light strikes the surface of the CCD chip, an electron is released in one of the pixels. As the integration continues, electrons accumulate in each pixel and are converted to intensity to form an image. According to Jeff Coughlin, a graduate of the Emory University Physics Department, up to 90%[10] of incident photons cause the release of an electron on a CCD, making CCD cameras much more sensitive than film, the previous method of light collecting, which has a conversion rate of only 2%.

However, like all forms of photography, noise is a main concern for the astronomer - if there is not a high enough signal to noise ratio (S/N), the images are unusable. There are three main sources of noise for a CCD camera that must be accounted for in order to make any observational data accurate and useful; calibration frames are taken at the end of each observing session and subtracted from each image frame taken during that session to eliminate this noise. The first calibration frame is a Bias Frame, used to offset any residual pixels that are not reset to zero after an image is captured. Bias frames have an exposure time of zero seconds. The second calibration frame is called the Dark Frame, which is used to subtract out any thermal photons emitted from the non-stellar sources. This occurs even though the camera is cooled to -30^{o} C and the Dark Frames are taken by exposing an image with the shutter of the camera closed. The Dark Frame must have an exposure that is as long as the longest image exposures of the observing session, as thermal photons accumulate on the CCD as long as an image is being taken. The final calibration frame is the Flat Frame, which is an exposure of an evenly illuminated source. This

[10] This percentage depends on the wavelength of light being captured and the CCD camera being used. For example, the SBIG ST10 XME can have up to 90% excitation of light at 540 nm.

frame both compensates for the fact that pixels do not all respond to photons at exactly the same rate and subtracts out any dust on the sensor (Kallrath and Milone 1999: 28-30) (Coughlin 2007:11-12).

Johnson/Bessel Filter Set

Astronomical objects can emit light in a wide range of wavelengths and it is necessary to have a many different filters for the camera so all the data can be collected. The use of five filters, Ultraviolet (U), Blue (B), Visual (V), Red (R), and Infrared (I) allow the camera to collect wavelengths of light from ~300 nm to ~1100 nm. Figure 6 identifies the range for each of the filters in the Johnson/Cousins UBVRI system. These are the standard filters used in astronomical observation. To give a basis for comparison, the visible spectrum spans approximately 400 nm to 750 nm. It is beneficial to collect many different wavelengths of light because it is possible that the binary system emits most of its energy in a very specific range on the spectrum. Therefore, some potentially pivotal data may not be collected if the entire spectrum is not recorded (Coughlin 2007: 6).

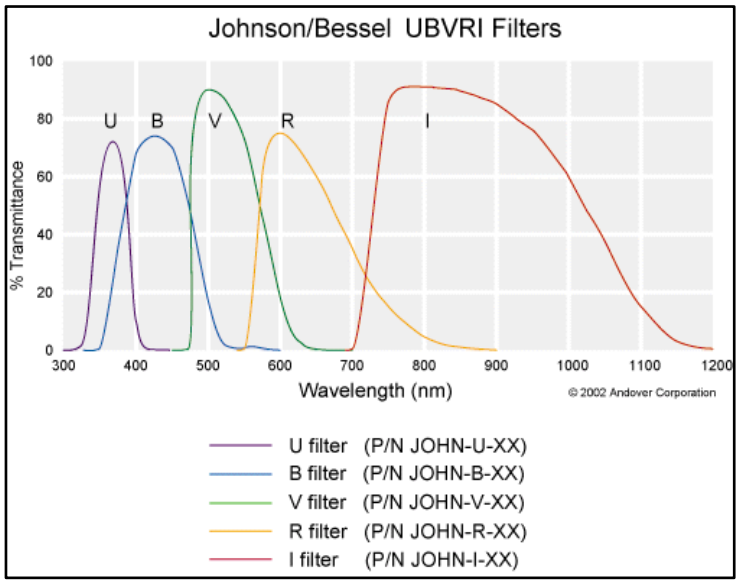

Figure 6: % Transmittance vs. Wavelength for each of the Johnson/Bessel filter set (Andover Corporation 2011)

Photometry

Once many observation sessions have been completed, differential photometry must be performed on the hundreds of images to obtain a light curve of the binary star system. Differential photometry is the method by which a camera measures the change in intensity of light (flux) emitted by an object. However, this light can be impacted by the Earth's atmosphere; as the object moves across the night sky, the light must travel through varying amounts of Earth's atmosphere (air mass). Furthermore, changes in cloud layer or wind can cause minor changes in the light being collected by the CCD. To correct for this, the observer compares the object to a reference star in the image, which is assumed to have a constant light intensity. Any fluctuations in the light due to changes in atmosphere conditions for this reference star are also taken into consideration for the object. This eliminates atmospheric disturbances in the field of view.

A third star, called the check star, is also needed to validate the observations for any given night. This check star is also in the field of view of the telescope with the reference star and object; it should also have a constant magnitude in order to verify the constancy of the reference star. The check star is also needed to measure any inherent variability in the images, as the standard deviation from the average of the check star will correlate to the object in question (Coughlin 2007: 12-13).

4 – OBSERVATIONS OF KR PERSEI

Research Background

According to Chen et al. KR Persei is a detached system consisting of two F5V spectral type stars with visual magnitude at approximately 10.5. Since the stars are nearly identical spectral types, and thus nearly the same temperature, the primary and secondary minimum should be almost identical. The period for this system is just under one day in length, which makes it difficult to obtain both primary and secondary minimum from the same location on Earth. However, there are two ways to obtain a full light curve. First, from one night to the next approximately five minutes of new light curve data can be obtained. Therefore if observations are spaced out over the course of several months, the entire light curve can be captured. However, this can be impractical as the seasons change. The second method is to collect data on the same nights at different locations on the Earth so that all parts of the light curve can be collected.

Observations

Observations of KR Per were taken with Emory Observatory's 24" telescope on the nights of September 13th, 14th, and 27th, October 1st, and 2nd, 2010 as well as January 22nd and 27th 2011. Data collected in 2010 used the Apogee AP47 CCD camera cooled to -30^{o} C while data collected in 2011 used the SBIG ST10 XME CCD chip cooled to -25^{o} C. 2010-11 Emory University data was combined with data taken by Dr. Richard Williamon at the Fernbank Observatory in Atlanta, Georgia, USA, as well as data taken by Dr. Kwan-Yu Chen at the Yunnan Observatory in Kunming, Yunnan, China, in 1985. Williamon obtained data on the primary minimum and Chen obtained data on the secondary minimum due to their different locations. They then combined their datasets to create a near complete light curve that was used

to obtain many astronomical quantities of KR Per. Their research culminated in a paper entitled *The Eclipsing Binary KR Persei*, published in the Astronomical Journal Vol 90, No 9 in September 1985. 2010-11 Emory University data was combined with data from Chen et al. (1985) to verify or improve the previously determined quantities from that paper.

Differential photometry was performed on the 2010-11 Emory University data using the aforementioned equipment and MaximDL software. KR Per was compared to the reference star GSC 2892-1153 and the check star for photometry was GSC 2892-1590 (Figure 7). Chen et al. (1985) performed differential photometry using BD +43 1017 as the reference star and BD +43 1016 as the check star. Reference stars were not photometrically calibrated and all times were corrected to HJD.

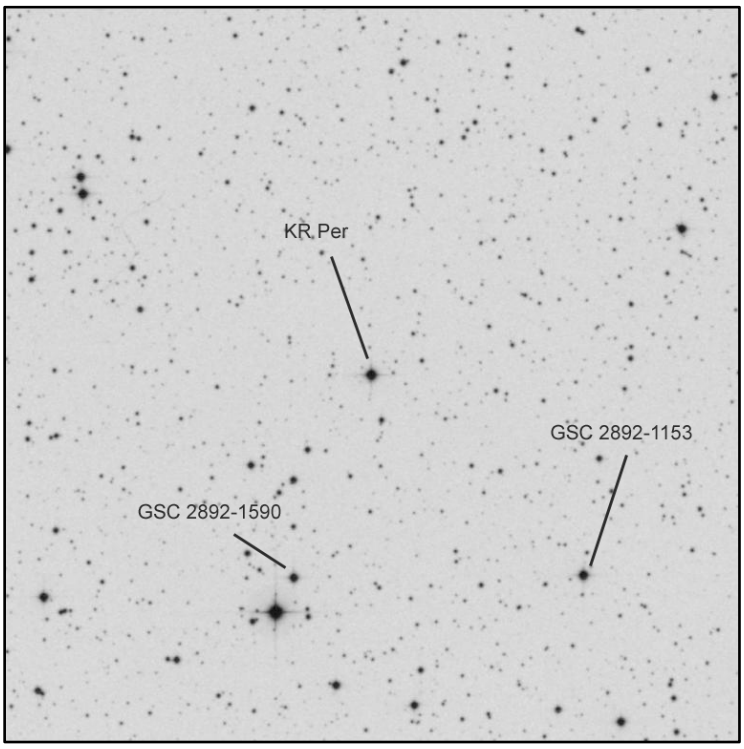

Figure 7: Field of view from the Apogee AP47 CCD at Emory University in Atlanta, GA, USA. Object, reference star, and check star for the 2010-11 Emory University data are identified

Minimum Timings and O-C Diagram

Table 1 shows the minimum timings for the 2010-11 Emory University data including errors, filters, and types of eclipse. Table 2 is a combination of both Chen et al. (1985) and 2010-11 Emory University data, which is used to compile an O-C diagram (Figure 8). To calculate the new ephemeris and O-C for the 2010-11 Emory University data the following equation was used: T_{min} = JD Hel. 2438048.3150 + 0.99607793 E_1 where E_1 is the epoch. This equation was used in the Chen et al. (1985) paper so it was required in order to add the 2010-11 Emory data correctly. Since no error was given from the Chen et al. (1985) data for the O-C diagram, a value of ±0.005 days was added to the figure. Figure 8 shows that the observed minus calculated value for the 2010-11 Emory University data is very small. These observation sessions are located on the far right of Figure 8. Having a small O-C value signifies that the times of minimums are very accurate. All other datapoints on Figure 8 are O – C values from Chen et al. (1985).

Table 1: Minimum Timings for KR Per (2010-11 Emory University)

T_{min} (JD Hel.)	Error (±)	Filter	Type
2455453.778654	0.000167	V	Pri
2455453.779201	0.000123	R	Pri
2455453.780121	0.000152	B	Pri
2455453.779000	0.000170	I	Pri
2455454.780684	0.000451	V	Pri
2455454.771624	0.001316	R	Pri
2455454.775624	0.000541	B	Pri
2455454.771143	0.001400	I	Pri
2455589.744694	0.000074	V	Sec
2455589.744789	0.001316	R	Sec
2455589.743896	0.000122	B	Sec

Table 2: Observed Minimum Times (JD Hel.), Observation Method/Filter (Ref.) Epoch (E), and Observed – Calculated value (O-C)

JD Hel. 2400000+	Ref.	E	(O-C)	JD Hel. 2400000+	Ref.	E	(O-C)
29491.537	ph1	-8590.5	0.029	38440.276	ph3	393.5	0.004
30234.562	ph1	-7844.5	-0.02	38441.279	ph3	394.5	0.011
30327.696	ph1	-7751	-0.019	38816.315	ph3	771	0.024
30377.565	ph1	-7701	0.046	39389.556	ph3	1346.5	0.022
30381.48	ph1	-7697	-0.023	39940.379	ph3	1889.5	0.014
30621.567	ph1	-7456	0.009	39941.337	ph3	1900.5	-0.024
30782.45	ph1	-7294.5	0.025	39946.353	ph3	1905.5	0.012
31075.269	ph1	-7000.5	-0.003	40149.553	ph3	2109.5	0.012
33949.436	ph2	-4115	-0.018	40150.54	ph3	2110.5	0.003
34663.61	ph2	-3398	-0.032	40151.54	ph3	2111.5	0.007
35718.484	v2	-2339	-0.005	41304.362	ph3	3269	-0.032
35721.485	v2	-2336	0.008	41350.313	ph3	3315	0
35722.474	v2	-2335	0.001	41549.538	ph3	3515	0.009
35743.381	v2	-2314	-0.01	41922.565	ph3	3889.5	0.005
35743.392	v2	-2313	0.005	41929.533	ph3	3896.5	0
35744.379	v2	-2311	0	41931.542	ph3	3898.5	0.017
35746.37	v2	-2309	-0.001	42303.539	ph3	4272	-0.021
35748.364	v2	-2308	-0.003	45311.7181	pe	7292	0.0029
35749.315	ph3	-2169.5	-0.009	45323.6712	pe	7304	0.0034
35887.297	ph3	-2163.5	-0.003	45324.667	pe y	7305	0.0028
35893.543	ph3	-1594	-0.024	45324.6668	pe b	7305	0.0026
36460.545	ph3	-1593	-0.018	45324.6672	pe u	7305	0.003
36461.555	ph3	-1211.5	-0.012	45348.0736	pe y	7328.5	0.0015
36841.542	ph3	-1206.5	-0.005	45248.0697	pe b	7328.5	-0.0024
36846.536	ph3	-1201.5	0.009	45348.0697	pe u	7328.5	-0.0024
36851.525	ph3	-435.5	0.002	45349.0664	pe y	7329.5	-0.0018
37614.447	ph3	-407.5	0.034	45349.0669	pe b	7329.5	-0.0013
37642.295	ph3	0	-0.02	45349.0657	pe u	7329.5	-0.0025
38048.553	ph3	193	-0.005	45350.0624	pe y	7330.5	-0.0018
38240.559	ph3	195	0.009	45350.0624	pe b	7330.5	-0.0018
38331.671	ph3	284.5	-0.028	45350.0619	pe u	7330.5	-0.0023
38373.531	ph3	326.5	-0.003	45351.5614	pe	7332.0	0.0031
38384.474	ph3	337.5	-0.017	55453.7787	pe v	17474.0	-0.0021
38385.47	ph3	338.5	-0.017	55453.7792	pe r	17474.0	-0.00155
38386.471	ph3	339.5	-0.013	55453.7801	pe b	17474.0	-0.00063
38387.488	ph3	340.5	0.009	55453.7790	pe i	17474.0	-0.00175
38399.42	ph3	352.5	-0.013	55454.7807	pe v	17475.0	-0.00386

JD Hel. 2400000+	Ref.	E	(O-C)	JD Hel. 2400000+	Ref.	E	(O-C)
38406.418	ph3	359.5	0.013	55454.7716	pe r	17475.0	-0.00520
38407.426	ph3	360.5	0.025	55454.7756	pe b	17475.0	-0.00120
38410.396	ph3	363.5	0.007	55454.7711	pe i	17475.0	-0.05684
38412.395	ph3	365.5	0.014	55589.7447	pe v	17610.5	-0.00069
38413.368	ph3	366.5	-0.01	55589.7448	pe r	17610.5	-0.00058
38439.292	ph3	392.5	0.016	55589.7439	pe b	17610.5	-0.00149

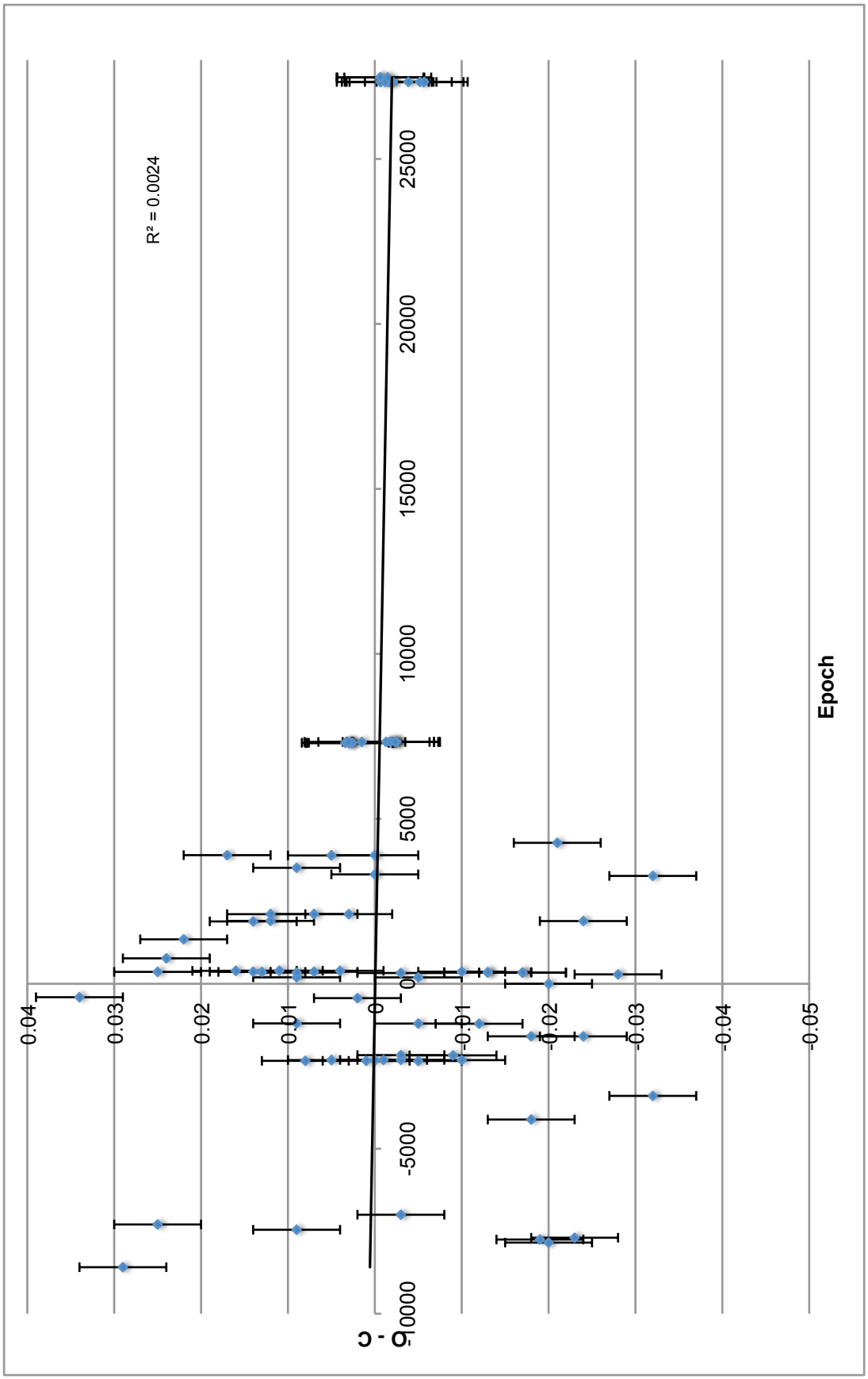

Figure 8: O – C Diagram for Chen et al. (1985) data and 2010-11 Emory data (far right)

Results

The purpose of this thesis is to reevaluate the astronomical quantities identified from the research performed by Chen et al. This reevaluation was performed using PERANSO period analysis software and Binary Maker 3. Since Chen et al. had obtained data using blue and visual filters, 2010-11 Emory University data was combined with that dataset for those filters. Chen et al. did not obtain a light curve with a red or infrared filters so any analysis of the red or infrared light curves was performed using only 2010-11 Emory University data. Table 3 identifies the specific period of KR Per by each filter type and data set. Table 4 identifies all of the astronomical quantities that Chen et al. calculated in their 1985 paper and Table 5 lists the orbital parameters that were calculated using all datasets, past and present.

Since no radial velocity curves are available for KR Per, all results in Table 5 are based on the results from Chen et al. For example, the mass ratio cannot be directly determined with radial velocity data so the value of 0.50 from Chen et al. (1985) was used to calculate other parameters.

Table 3: Period Length by Dataset (Chen designates Chen et al. data)

Filter	**Dataset**	**Period (days)**	**Period (sec)**
V	Emory	0.996087	86061.9168
	Emory + Chen	0.996077	86061.0528
B	Emory	0.996069	86060.3616
	Emory + Chen	0.996077	86061.0528
R	Emory	0.996079	86061.2256
I	Emory	0.996081	86061.3984
U	Chen	0.996095	86062.6080
All	*All data*	*0.996081*	*86061.3737*

Table 4: Orbital Parameter Solutions for KR Per from Chen et al. (1985)

Parameter	Value
Period (sec)	86061.13315
Inclination (^{o})	83.7
Mass Ratio (m_{sec}/m_{pri})	0.50 or 0.43
Radius Ratio (R_{sec}/R_{pri})	0.96
Spectral class of both stars	F5V
Fractional Radius of Primary	0.324
Fractional Radius of Secondary	0.311
Eccentricity[11]	0.009
Longitude of Periastron (ω)[12]	160^o

Table 5: Orbital Parameter Solutions for KR Per from 2010-11 Emory U. and Chen et al. data

Parameter	Value
Period (sec)	86061.3737
Inclination (^{o})	83.7
Mass Ratio (m_{sec}/m_{pri})	~0.50
Radius Ratio (R_{sec}/R_{pri})	~0.96
Temperature Ratio (T_{sec}/T_{pri})	~0.993
Fill Factor of Primary	-0.042
Fill Factor of Secondary	-0.219
Fractional Radius of Primary	0.324
Fractional Radius of Secondary	0.311
V Eclipse Depth Ratio	0.99903
B Eclipse Depth Ratio	0.99486
R Eclipse Depth Ratio	0.99964
Luminosity Ratio	0.9216

Light Curves and Modeling

This section includes the final light curves for all filter types and all datasets as well as two-dimensional and three-dimensional modeling of KR Per in Binary Maker 3. Figure 9 was created to identify the characterization of KR Per using all datasets. The figure shows that KR Per is a detached system, which is consistent with Chen et al. The fill factor of the primary and secondary star inside the Roche lobe is -0.042 and -0.219, respectively. Figure 10 is a three-

[11] Amount by which an orbit deviates from its circular path (Carroll and Ostlie 2007: 26)
[12] Longitude of the closest approach to the center of mass (Carroll and Ostlie 2007: 26)

dimensional model of KR Per in three different phases of its orbit. Figure 11 combines both Chen et al. and 2010-11 Emory University data into single light curves by filter type in PERANSO.

It should be noted that Chen et al. performed their analysis on their light curves in relative flux in lieu of magnitudes (differential photometry was performed using a reference star at magnitude 0.0 instead of a specific value). Therefore, when 2010-11 Emory University and Chen et al. (1985) data were combined, the differential values between shoulder sections needed to be added to Chen et al. (1985) data to allow the two datasets to be combined for analysis.

Figures 12, 14, and 16 are the individual light curves for B, V, and R with a computer model from BM3. The computer model was obtained using the inclination, fractional radii of the components, and mass ratio from the Chen et al. (1985) paper. The temperature of each component was varied so that the computer model would best fit the observed light curve. Figures 13, 15, and 17 have identical parameters to Figures 12, 14, and 16, respectively except that the light curve is modified by adding a reflection value. The quantitative values for each dataset can be found in the table below each two-figure set.

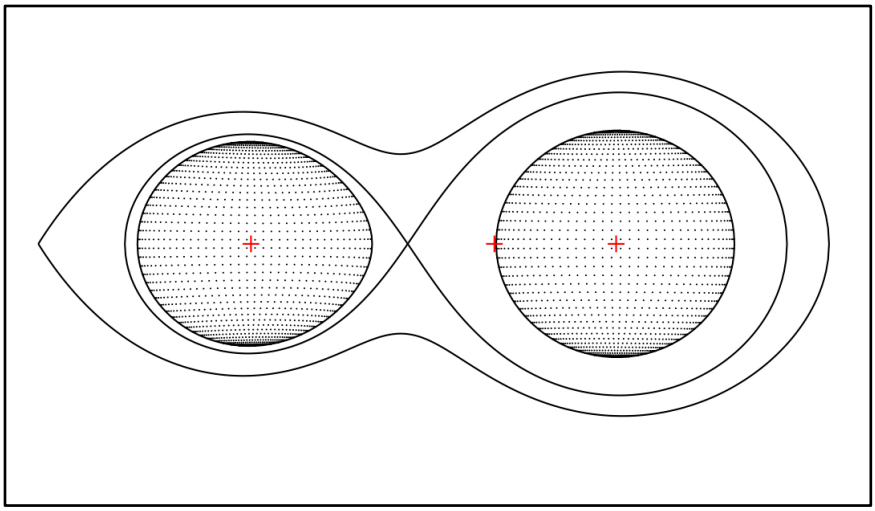

Figure 9: Geometrical model of KR Per system. The cross signs represent the center of mass for each star and the center of mass of the system (more central cross). The inner solid black line represents the Roche Lobe for each star. The primary star is on the right. Binary Maker 3 confirmed that this system is detached.

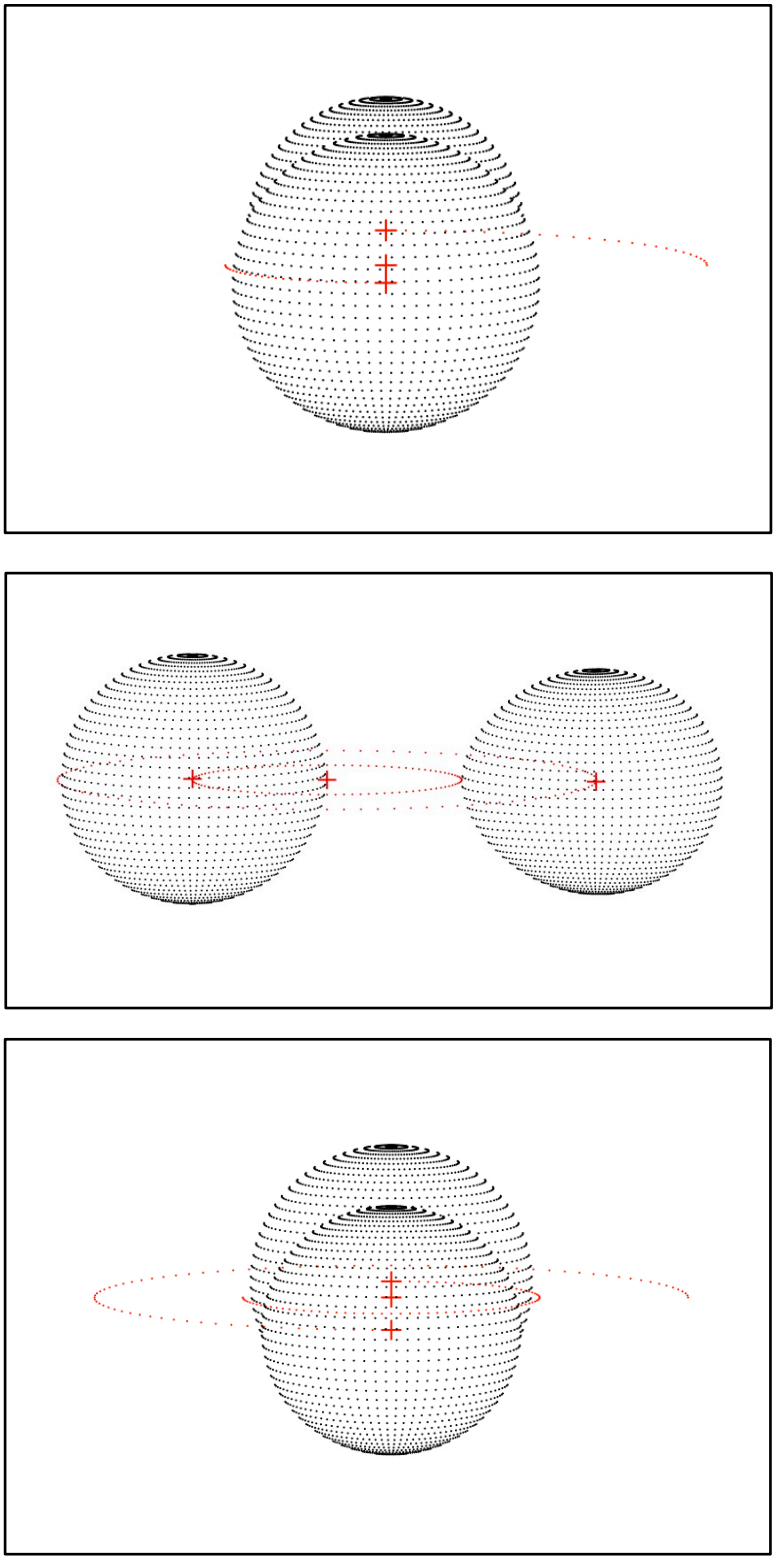

Figure 10: Three-dimensional model of the KR Per system orbit at phase 0.00 (top), 0.25 (middle), and 0.50 (bottom).

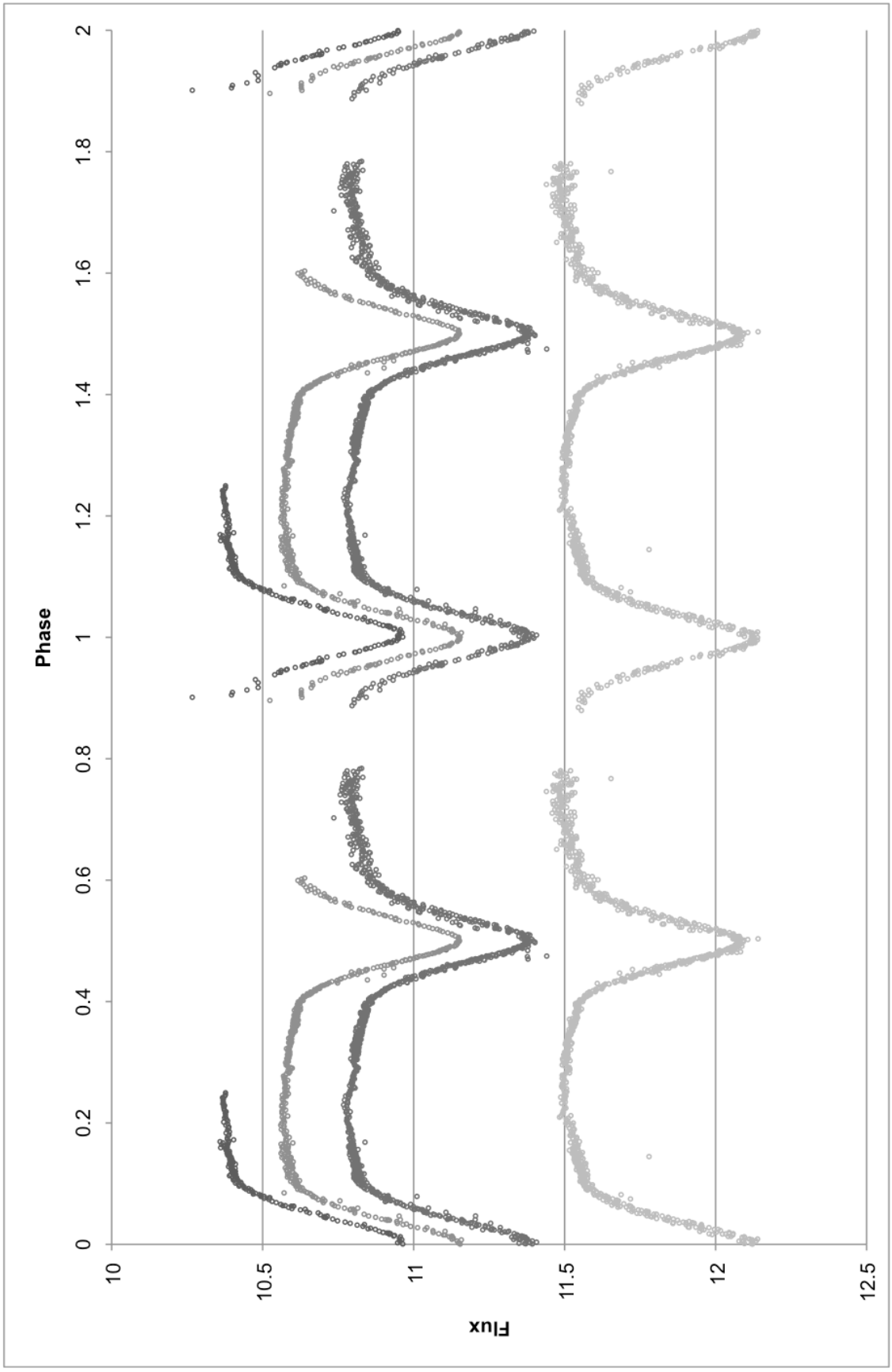

Figure 11: Top to bottom: I, R, V, and B light curves (circles) for KR Per using 2010-11 Emory University and Chen et. al data

Computer Modeling

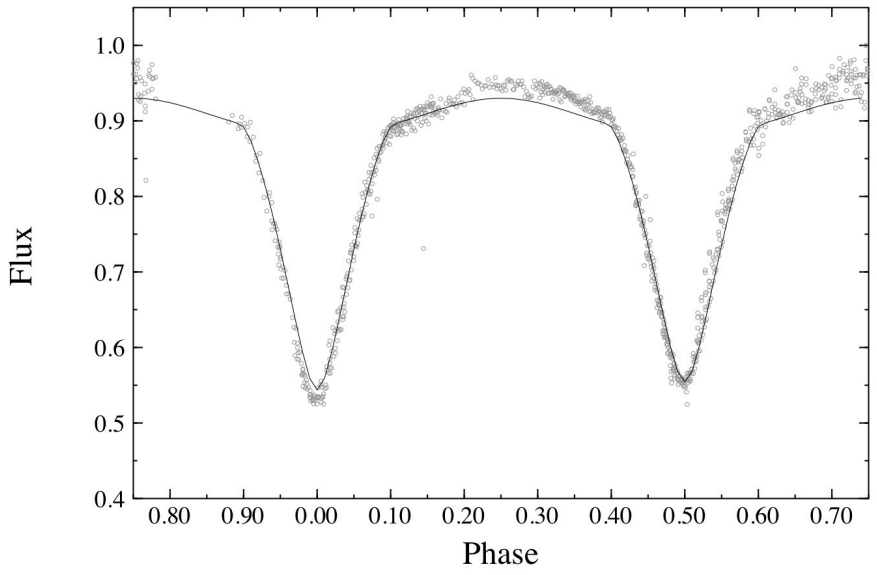

Figure 12: Blue light curve (circles) with Binary Maker 3 model without inclusion of reflection effect.

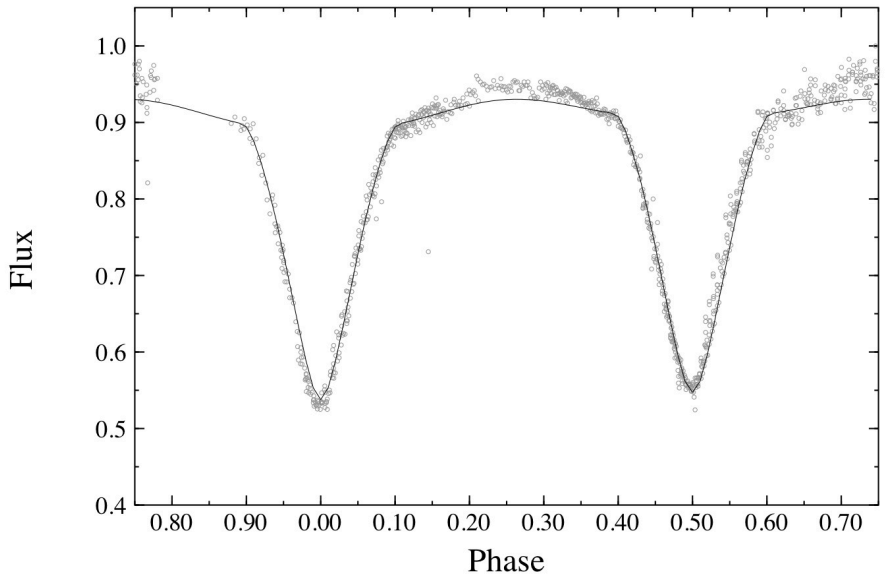

Figure 13: Blue light curve (circles) with Binary Maker 3 model with theorized reflection effect.

Table 6: Parameters for Figure 13 in BM3

Normalization Factor	0.93
Temperature 1	5350 K
Temperature 2	5300 K
Wavelength	4400 Å
Reflection 1	0.5
Reflection 2	1.0

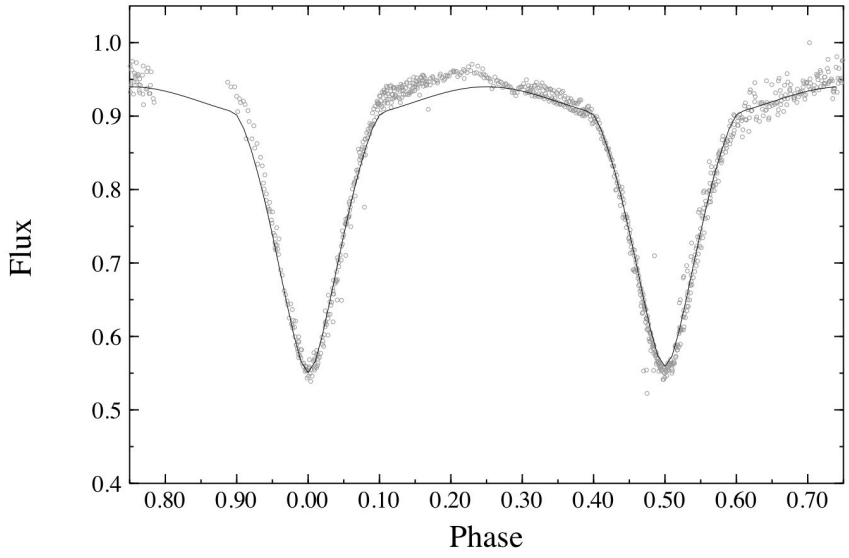

Figure 14: Visual light curve (circles) with Binary Maker 3 model without inclusion of reflection effect.

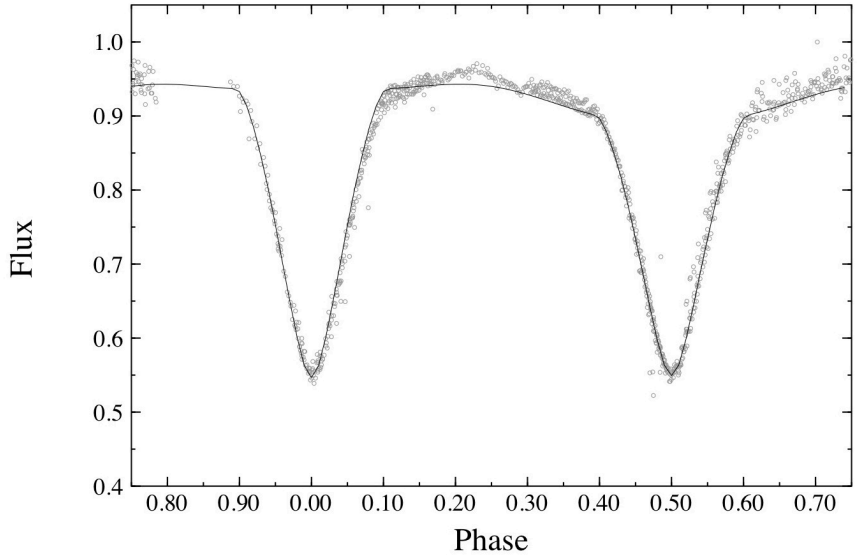

Figure 15: Visual light curve (circles) with Binary Maker 3 model with theorized reflection effect.

Table 7: Parameters for Figure 15 in BM3

Normalization Factor	0.94
Temperature 1	5350 K
Temperature 2	5300 K
Wavelength	5500 Å
Reflection 1	2.0
Reflection 2	0.5

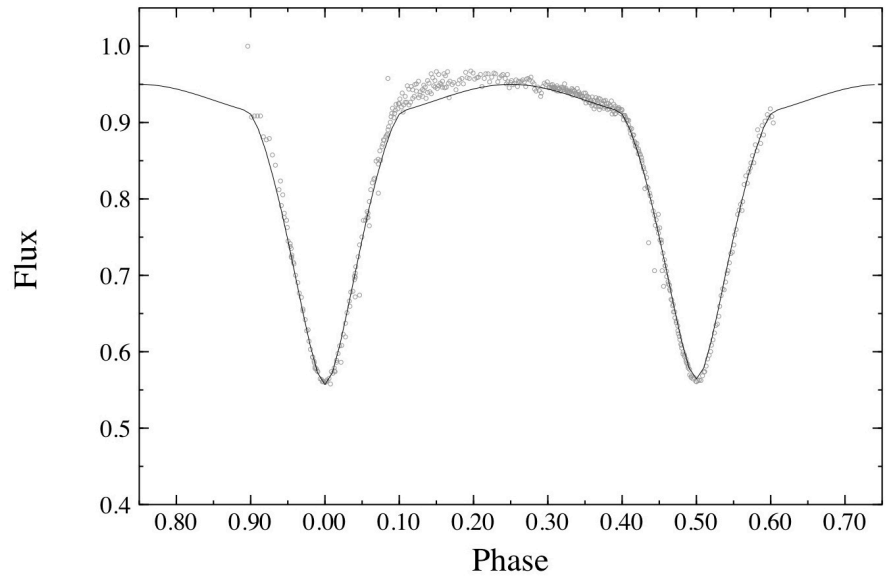

Figure 16: Red light curve (circles) with Binary Maker 3 model without inclusion of reflection effect.

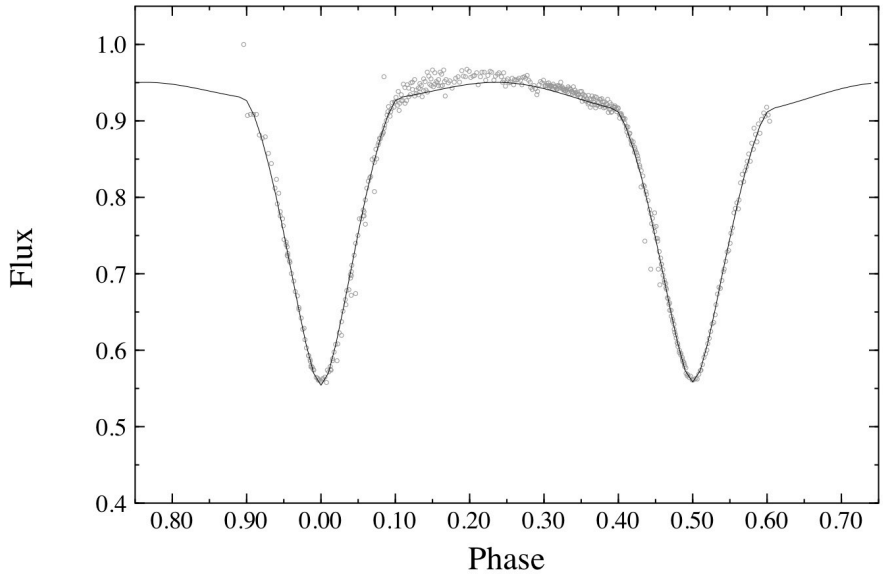

Figure 17: Red light curve (circles) with Binary Maker 3 model with theorized reflection effect.

Table 8: Parameters for Figure 17 in BM3

Normalization Factor	0.95
Temperature 1	5350 K
Temperature 2	5300 K
Wavelength	6500 Å
Reflection 1	1.2
Reflection 2	0.5

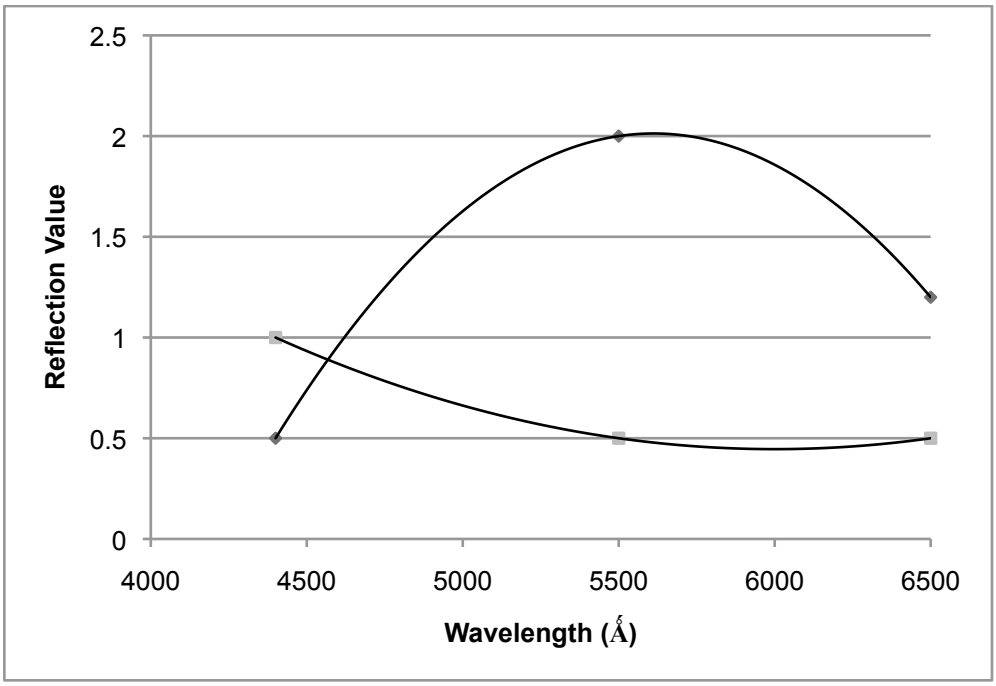

Figure 18: Reflection values from Tables 6, 7, and 8 vs. wavelength of filter in angstroms. 4400 – Blue, 5500 – Visual, 6500 – Red. Diamonds are Reflection 1 (primary component). Squares are Reflection 2 (secondary component).

5 – DISCUSSIONS AND CONCLUSIONS

According to the 2010-11 Emory University data, KR Per has not changed over the 26 years since Chen et al. performed their observations on the system. Thanks to modeling in BM3, it appears that KR Per is still a detached system (see Figure 9), has a radius ratio of 0.96, and still has an orbital inclination of 83.7^{o}. Furthermore, the light curves for the 1985 data and the 2010-11 data appear identical and the period determined from 2010-11 Emory University data is identical to the period from Chen et al. (1985) (Table 3). Furthermore, the fact that 2010-11 Emory University data and Chen et al. (1985) data could be so easily combined into I, V, B, and R light curves further solidifies the conclusion that this system has not changed (Figure 11).

Some of the results that Chen et al (1985) identified do not agree with the results from this thesis when the combined datasets were analyzed. First, Chen et al. determined that there is a possible eccentricity of 0.009 with a longitude of periastron of 160^{o}. This eccentricity is very small and considering the data used for that paper, it is unlikely that it can be directly verified. When the 2010-11 Emory University data was combined with Chen et al. (1985) data, it appears that no eccentricity exists as the period and primary and secondary minimums have not changed. Therefore, Table 5 omits any eccentricity and longitude of periastron.

Second, Chen et al. classified both components of KR Per to be F5V stars with temperatures of ~6650 K. In order to determine this, the B – V values outside of eclipse must equal +0.44 according to previously determined stellar data[13] (Carroll and Ostlie 2007: Appendix G). It is unclear how Chen et al. arrived at the conclusion that this system has two F5V components because their B – V value was +0.24 which according to stellar data would classify these components as A8 stars (Chen et al. 1985: 1859). Furthermore, once the 2010-11 Emory

[13] B – V is the difference in flux between the blue filter light curve and the visual filter light curve.

University data was combined with Chen et al. (1985), the B – V value was +0.75, which would classify each component as a G8 star (T_{eff} = ~5310 K) (Carroll and Ostlie 2007: Appendix G). Therefore, Table 5 omits the stellar classification of the components, as with the currently available data, it is not possible to make specific mass or temperature determinations. The only way to derive specific masses and temperatures is to obtain radial velocity curves from stellar spectra. It is possible that Chen et al. were in error when they assigned each component of KR Per an F5V designation. If the stars in KR Per were both G8, this would agree mathematically with the theory that this system includes a multiple reflection effect.

There is a strong possibility of a multiple reflection effect between the two components. The term multiple reflection effect means "the first star heats the second star, and the (now warmer) second star then heats the first star more than otherwise expected because of its own raised temperature" (Kallrath and Milone 1999: 99). Figures 12 through 18 and Tables 6 through 8 outline BM3 modeling of the data that is used to support this conclusion. According to Kallrath and Milone (1999), a single reflection effect can cause the light curve to rise in the shoulder region outside of the secondary eclipse. Multiple reflections can cause both the primary and secondary shoulder regions to be altered.

When one star heats a companion star, the companion will get hotter and hotter and eventually reach the Eddington Limit[14] and have mass loss unless the heat is distributed elsewhere in the star. KR Per does not show mass loss in any of the observations because if there was, the angular momentum of the system would have changed, thereby altering the period. However, over the past 26 years, the period of KR Per has not changed at all and as a result, this added heat from the multiple reflection effect must be distributed elsewhere by the stars.

[14] Derived from the Eddington Theory, which states that there is a specific point where the gravitational force inward equals the radiative force outward. If the limit is exceeded, a mass loss from the star occurs to maintain the balance of forces (Carroll and Ostlie 2007: 341).

For this theory to be viable the primary star must have a large convection zone and the secondary star must have a large radiative zone. The convection zone of a star is the range of radii in a star in which energy is transported by convection. In the case of KR Per, the primary has a large convection zone due to its higher density and is distributing the new heat away from the face directed at the secondary. Alternatively, the radiative zone of a star is the area where energy is expelled from the star in the form of electromagnetic waves (Carroll and Ostlie 2007: 255-258). The secondary star of KR Per appears to be very radiative, due to its shallow convection zone, that expels heat onto its companion.

Support for this conclusion can be drawn from observations of the data and the computer modeling in BM3. Figures 13, 15, and 17 show that when a reflection value is added to the BM3 modeling, the theoretical curves correlate much better to the observed light curves. Second, the data from Chen et al. (1985) in tandem with 2010-11 Emory University data, confirms this reflection effect even after 26 years. Third, this would help explain why the primary and secondary eclipse depths are so similar. In Table 5, the eclipse depth ratios for V, B, and R are 0.99034, 0.994860 and 0.99641, respectively. If the secondary star in KR Per truly is half the mass of the primary, this reflection effect would help explain why the temperature ratio is ~1 and why the eclipse depths are almost identical.

This theory can also be conceptualized from the light curve data. As KR Per comes out of primary eclipse, the primary star is cooler at 4400 angstroms on the side facing the secondary star. As it enters and exits secondary eclipse, the secondary star is hotter on that face, again in 4400 angstroms. This is observed in Figure 13, as the shoulder region is lower coming out of primary minimum and higher around the secondary minimum. As the datasets increase in wavelength (to 5500 angstroms and 6500 angstroms), the stars' reflection effects are reversed

and the primary star is hotter as it exits primary while the secondary is cooler as it exits secondary (see Figures 15 and 17). Figure 18 graphically depicts the reflection values vs. filter wavelength for the previous graphs and tables.

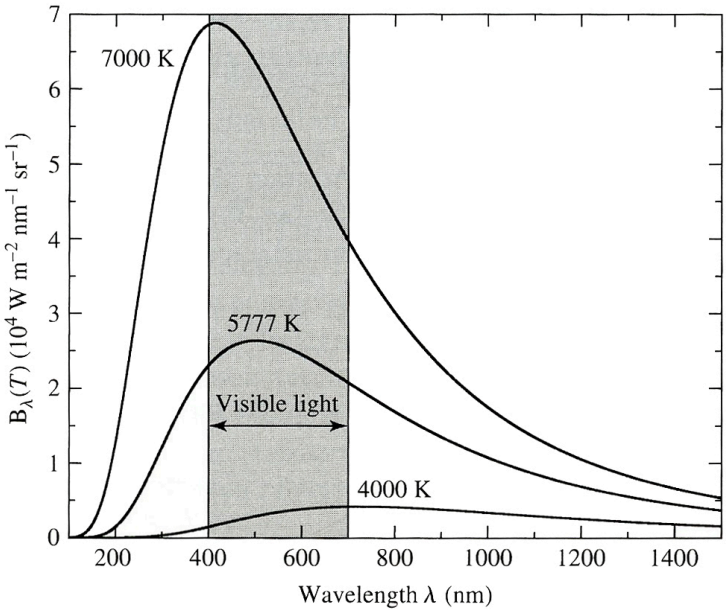

Figure 19: Planck Distribution shows similarities to the reflection value vs. wavelength graph (Figure 18). As temperature increases, the peak for $B_\lambda(T)$ increases but the wavelength of light at which the peak occurs decreases (Carroll and Ostlie 2007: 69)

Figure 19 has a strong geometrical correlation to a Planck Distribution because the reflection value also appears to be dependent on wavelength. The primary star has a peak reflection value at ~5600 angstroms. The secondary does not show a peak but since the trendline is increasing as wavelength decreases, it can be hypothesized that there is a peak for the secondary's reflection value between 3000 and 4000 angstroms. Finally, as previously stated, the B – V value for KR Per appears to make each component a G8 star (t = 5310 K). If this were the case, then Wien's displacement law[15] would show that the maximum amount of energy that can be radiated would be at ~5460 angstroms for the primary star. Considering the reflection value

[15] Dictates that there is a specific relationship between the maximum wavelength of energy that an object can emit and the temperature of the object. The mathematical equation is: λ_{max} T = 0.002897755 m K

peaks at ~5500 angstroms, mathematically the primary being a G8 type star is ideal and the secondary would also be a G8 star due to the similar eclipse depths[16].

Another way to model this multiple reflection effect is to use Binary Maker 3 and add one spot to each component (Figure 20). A spot on a star is an area of increased magnetic activity (like a sunspot on our Sun) and has a cooler temperature than the surrounding area. However, it is possible to give spots a *higher* temperature in BM3, thereby simulating the temperature increase due to the multiple reflection effect[17]. In BM3, two spots with arbitrary radii of 20^o (angular size of a starspot in degrees) were placed at zero longitude and 90^o colatitude so that they face one another as the stars orbit. The temperature of the spot on the primary component is 20% hotter than t_{pri} of 5350 K and the temperature of the spot on the secondary component is 10% hotter than t_{sec} of 5300 K. This method of modeling creates a very similar curve to Figure 15 (spot modeling used the V light curve) because the reflection effect is now being replaced with a hotter spot. Therefore, spot modeling agrees with the previous analysis that a mu1ltiple reflection effect exists in the KR Per system.

[16] With the data currently accessible, BM3 only uses the ratio t_{pri}/t_{sec} when creating a computer model. Therefore, as long as the ratio stays the same, any temperatures can be used (e.g. temperature of a G8 star).
[17] I am using the spot feature of BM3 to approximate a multiple reflection effect in KR Per and not to add a real starspot to each component.

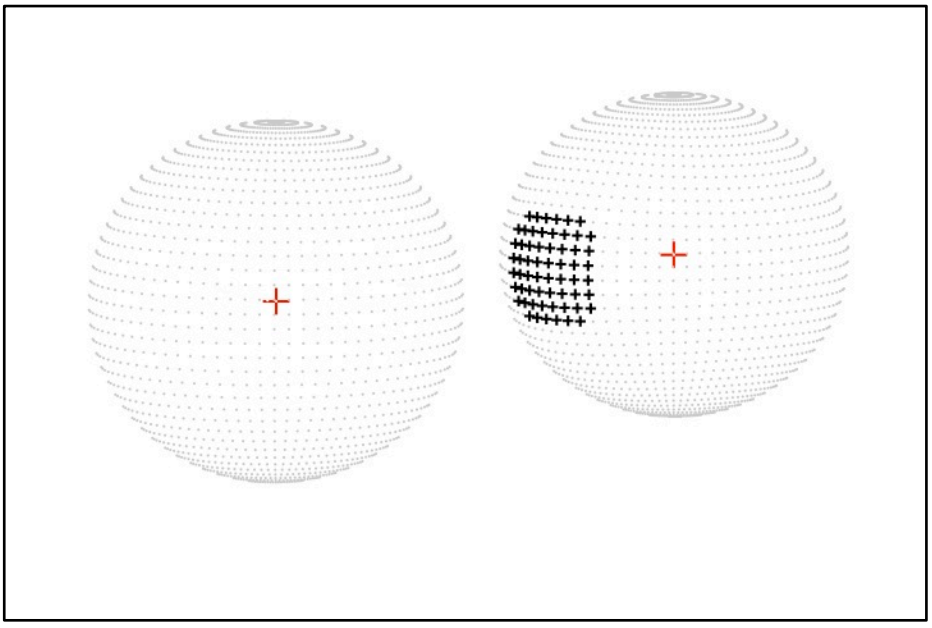

Figure 20: Three-dimensional model of KR Per with 1 spot on each of the components at 0 longitude, 90^{o} colatitude, with spot radii of 20. The temperature for the spot on the primary star is 20% hotter than t_{pri} and the spot on the secondary is 10% hotter than t_{sec}. Spot on secondary star is shown in deep black.

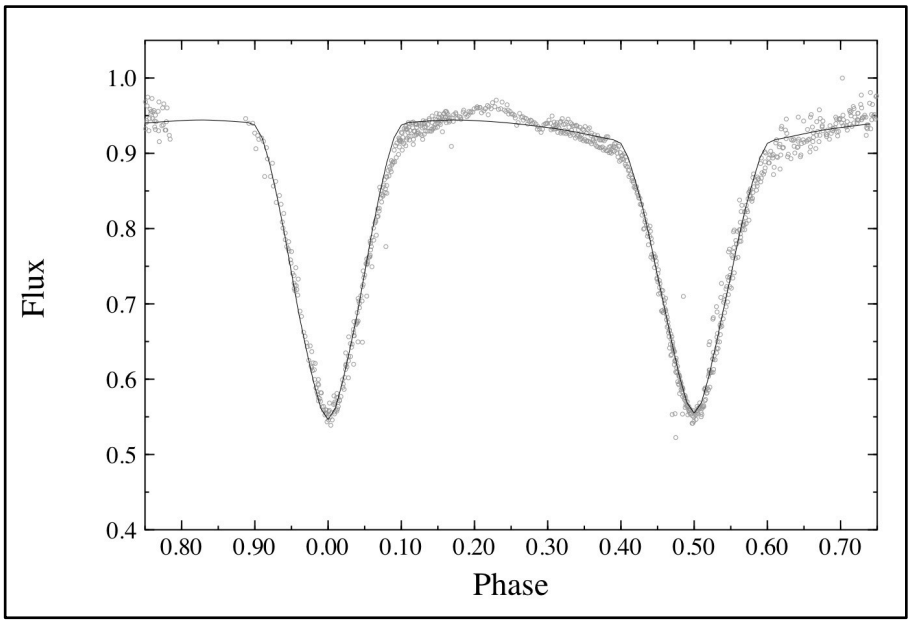

Figure 21: Visual light curve (circles) with two spot modeling (solid line) in BM3. This figure can be directly compared to Figure 15.

The next obvious step in the analysis of KR Per should be to obtain line spectra and radial velocity curves for the system. The radial velocity curves are essential for identifying the specific masses, temperatures, and radii of each component star and having the line spectra could support the theory that KR Per has a multiple reflection effect. If the spectral lines broaden (thicken) as the primary star exits primary eclipse, it can be concluded that the pressure on the face of the primary star is greater than expected. This increased pressure is caused by an increased temperature on that face as a result of the multiple reflection effect.

In the following weeks, it is my goal to work with more complex modeling code at the Georgia Institute of Technology. There, Dr. James Sowell, Senior Academic Professional in the Physics Department, is very knowledgeable in Wilson-Devinney (WD) coding. WD can accurately model almost any eclipsing binary system and has more unique solving abilities than BM3 thanks to continuous updating of the physics underlying the code. However, more data is still needed to obtain any specific values for many of the astronomical quantities listed in Table 5. If a future researcher obtains stellar spectra and radial velocity curves for KR Per, many of the hypotheses presented in this thesis may be answered - and a final solution for this binary system could be discovered.

REFERENCES

Andover Corporation. 2011. Images. Johnson/Bessel UBVRI Filters. Salem, New Hampshire.

Carroll, B. W. Ostlie D. A. 2007. An Introduction to Modern Astrophysics Second Edition. San Francisco: Pearson Education Inc.

Chen, K-Y., Williamon, R. M., Liu, Q., Yang, Y. and Lu, L. 1985. The Eclipsing Binary KR Persei. The Astronomical Journal 90.9: 1855-1859.

Coughlin, J. L. 2007. Observations and Models of Eclipsing Binary Systems. Atlanta: Emory University Library.

Dhillon, Vik. 2010. Cassegrain Telescope Diagram. Teaching Telescopes. Sheffield, England.

Goddard Space Flight Center. 2011. HR-Diagram. Life Cycles of Stars. Teachers' Corner. Greenbelt, Maryland.

Kallrath, J. and Milone, E. F. Eclipsing Binary Stars: Modeling and Analysis. 1999. New York: Springer-Verlag New York, Inc.

Wilson, R.E. Accuracy and Efficiency in the Binary Star Reflection Effect. 1990. The Astrophysical Journal 356: 613-622.